What is measured in the scanning gate microscopy of a quantum point contact?

Rodolfo A. Jalabert,[1] Wojciech Szewc,[1] Steven Tomsovic,[2,*] and Dietmar Weinmann[1]

[1] *Institut de Physique et Chimie des Matériaux de Strasbourg, UMR 7504, CNRS-UdS, 23 rue du Loess, BP 43, 67034 Strasbourg Cedex 2, France*

[2] *Department of Physics, Indian Institute of Technology Madras, Chennai, 600 036 India*

(Dated: October 13, 2010)

The conductance change due to a local perturbation in a phase-coherent nanostructure is calculated. The general expressions to first and second order in the perturbation are applied to the scanning gate microscopy of a two-dimensional electron gas containing a quantum point contact. The first-order correction depends on two scattering states with electrons incoming from opposite leads and is suppressed on a conductance plateau; it is significant in the step regions. On the plateaus, the dominant second-order term likewise depends on scattering states incoming from both sides. It is always negative, exhibits fringes, and has a spatial decay consistent with experiments.

PACS numbers: 85.35.Ds, 07.79.-v, 73.23.-b, 72.10.-d

Scanning gate microscopy (SGM) has been intensively used during the past decade to investigate electronic transport in nanostructured two-dimensional electron gases such as quantum point contacts [1–4], quantum billiards [5], and rings [6, 7]. In this technique, a charged tip that locally influences a device's electrons is scanned over the surface; i.e. the perturbed nanostructure's conductance is a function of the tip position. The SGM technique is of great fundamental interest since it provides a wealth of data that depends on the microscopic electron transport. It can generate very detailed sample characterization and more precise information of the disorder configuration than a traditional transport measurement.

Of importance in SGM studies is the precise physical interpretation of data. Are the measurements sensitive to the electron flow as often just stated or, perhaps, the local electron density? Whereas experiments and numerical simulations have yielded conductance change patterns caused by local perturbations closely related to calculated electron flows or local electron densities [2, 3, 6–10], the precise relationships among these quantities and interpretations remain far from obvious. Moreover, it is recognized that in a linear response framework the current density is not uniquely defined, and its study merely provides a way to visualize the structure of the scattering states at the Fermi energy [11]. Thus, our goal is to provide a clear-cut relationship between the conductance change in a SGM setup and the unperturbed scattering states which is valid for an arbitrary coherent structure.

Consider a system with a Hamiltonian $H = H_0 + V$, where H_0 represents the unperturbed structure and V the tip potential. Though quite general, the main focus is on a quantum point contact (QPC). This paradigm exhibiting conductance quantization [12–16] has been well studied by SGM [1–4]. In addition, recent work suggests the relevance of this powerful technique for probing the nonlocality of electronic interactions [17–19].

The scattering theory of quantum conductance [20, 21] assumes that the leads are disorder-free, confined in the transverse (y) direction, and semi-infinite in the longitudinal (x) direction. The electron states in the leads are products of quantized transverse wavefunctions $\phi_a(y)$ labeled by the index a with transverse energy $\varepsilon_a^{(\mathrm{t})}$ and plane waves propagating in the x direction with wavevector magnitudes k_a. The total electron energies are $\varepsilon = \varepsilon_a^{(\mathrm{t})} + \hbar^2 k_a^2/2M$, with M the effective electron mass. The N transverse momenta which satisfy this relationship with $k_a^2 > 0$ define the $2N$ propagating channels of the leads with energy ε. Denoting $\mathbf{r} = (x, y)$, the incoming (-) and outgoing (+) lead states are defined as

$$\varphi^{(\pm)}_{1,\varepsilon,a}(\mathbf{r}) = \frac{\exp(\mp i k_a^{\pm} x)}{\sqrt{2\pi\hbar^2 k_a/M}}\, \phi_a(y)\ , \quad x < 0\ . \tag{1}$$

For $x > 0$, the index $1 \to 2$ and the opposite sign is taken in the argument of the exponential. An infinitesimal negative (positive) imaginary part is given to k_a for incoming (outgoing) lead states. For simplicity, consider a confining potential that is x-independent in the asymptotic region even though any separable potential can be treated if allowance is made for an x dependence of k_a.

The scattering states corresponding to an electron incoming from the left lead 1 (right lead 2) with energy ε in the mode a are given in the asymptotic regions by

$$\begin{aligned}
\Psi^{(+)}_{1,\varepsilon,a}(\mathbf{r}) &= \begin{cases} \varphi^{(-)}_{1,\varepsilon,a}(\mathbf{r}) + \sum_{b=1}^{N} r_{ba}\varphi^{(+)}_{1,\varepsilon,b}(\mathbf{r}), & x < 0 \\ \sum_{b=1}^{N} t_{ba}\varphi^{(+)}_{2,\varepsilon,b}(\mathbf{r}), & x > 0 \end{cases} \\
\Psi^{(+)}_{2,\varepsilon,a}(\mathbf{r}) &= \begin{cases} \sum_{b=1}^{N} t'_{ba}\varphi^{(+)}_{1,\varepsilon,b}(\mathbf{r}), & x < 0 \\ \varphi^{(-)}_{2,\varepsilon,a}(\mathbf{r}) + \sum_{b=1}^{N} r'_{ba}\varphi^{(+)}_{2,\varepsilon,b}(\mathbf{r}), & x > 0 \end{cases}
\end{aligned} \tag{2}$$

Then the $2N\times 2N$ scattering matrix S, relating incoming and outgoing fluxes, can be written in terms of the $N\times N$ reflection and transmission matrices from lead 1 (2) as

$$S = \begin{pmatrix} r & t' \\ t & r' \end{pmatrix}\ . \tag{3}$$

The chosen lead state normalization corresponds to an incoming flux e/h and ensures the orthonormality of the

scattering states [20, 21]. The zero-temperature conductance of the unperturbed structure in units of the conductance quantum $2e^2/h$ is given by $g^{(0)} = \mathrm{Tr}[t^\dagger t]$, where Tr denotes the trace over the modes.

The Lippmann-Schwinger equation for the perturbed wave function $\chi^{(+)}_{l,\varepsilon,a}(\mathbf{r})$ using the retarded Green function $\mathcal{G}^{(0)}$ associated to H_0 is

$$\chi^{(+)}_{l,\varepsilon,a}(\mathbf{r}) = \Psi^{(+)}_{l,\varepsilon,a}(\mathbf{r}) + \int \mathrm{d}\bar{\mathbf{r}}\ \mathcal{G}^{(0)}(\mathbf{r},\bar{\mathbf{r}},\varepsilon) V(\bar{\mathbf{r}}) \chi^{(+)}_{l,\varepsilon,a}(\bar{\mathbf{r}})\ . \tag{4}$$

It is consistent within linear response theory to calculate the conductance change beginning with the current change carried by $\Psi^{(+)}_{1,\varepsilon,a}(\mathbf{r})$ with the spectral decomposition of $\mathcal{G}^{(0)}$ in the scattering wave-function basis. To first order in V, the integration over a cross section $\mathcal{S}_x$ on the scatterer's right [22] gives

$$I^{(1)}_{1,\varepsilon,a}(x) = \frac{e\hbar}{M}\ \mathrm{Im}\left\{ \int_{\varepsilon_1^{(\mathrm{t})}}^{\infty} \frac{\mathrm{d}\bar{\varepsilon}}{\varepsilon^+ - \bar{\varepsilon}} \sum_{\bar{l}=1}^{2} \sum_{\bar{a}=1}^{\bar{N}} Z^{1,\bar{l}}_{a,\bar{a}}(\varepsilon,\bar{\varepsilon})\ \mathcal{V}^{\bar{l},1}_{\bar{a},a}(\bar{\varepsilon},\varepsilon) \right\}, \tag{5}$$

where the matrix element of the perturbing potential in the scattering state basis is

$$\mathcal{V}^{\bar{l},l}_{\bar{a},a}(\bar{\varepsilon},\varepsilon) = \int \mathrm{d}\mathbf{r}\ \Psi^{(+)*}_{\bar{l},\bar{\varepsilon},\bar{a}}(\mathbf{r})\ V(\mathbf{r})\ \Psi^{(+)}_{l,\varepsilon,a}(\mathbf{r})\,. \tag{6}$$

In addition, a shorthand notation is introduced for the following quantities involving the unperturbed states:

$$Z^{1,1}_{a,\bar{a}}(\varepsilon,\bar{\varepsilon}) \ = \ \frac{iM}{2\pi\hbar^2} \sum_{b=1}^{\hat{N}} \left(\sqrt{\frac{\bar{k}_b}{k_b}} + \sqrt{\frac{k_b}{\bar{k}_b}} \right) t^*_{ba} t_{b\bar{a}} \exp\left[i(\bar{k}_b^+ - k_b^-)x \right], \tag{7}$$

$$Z^{1,2}_{a,\bar{a}}(\varepsilon,\bar{\varepsilon}) \ = \ \frac{iM}{2\pi\hbar^2} \left\{ \left(\sqrt{\frac{k_{\bar{a}}}{\bar{k}_{\bar{a}}}} - \sqrt{\frac{\bar{k}_{\bar{a}}}{k_{\bar{a}}}} \right) t^*_{\bar{a}a} \exp\left[-i(\bar{k}_{\bar{a}}^- + k_{\bar{a}}^-)x \right] + \sum_{b=1}^{\hat{N}} \left(\sqrt{\frac{\bar{k}_b}{k_b}} + \sqrt{\frac{k_b}{\bar{k}_b}} \right) t^*_{ba} r'_{b\bar{a}} \exp\left[i(\bar{k}_b^+ - k_b^-)x \right] \right\},$$

with $\hat{N} = \min\{N, \bar{N}\}$.

The $\bar{\varepsilon}$ integral of Eq. (5) has a principal part and a δ-function contribution. Since the current correction has to be independent of x, the integral can be evaluated in the limit $x \to \infty$. The principal part contribution is simply equal to that of the δ-function contribution. The result is thus for $\bar{\varepsilon} = \varepsilon$, and forthwith the energy arguments are dropped. The current change associated with the mode a at energy ε is given by

$$I^{(1)}_{1,\varepsilon,a} = \frac{e}{\hbar}\ \mathrm{Im}\left\{ \left(t^\dagger t\ \mathcal{V}^{1,1} - r^\dagger t'\ \mathcal{V}^{2,1} \right)_{a,a} \right\}. \tag{8}$$

The first term vanishes when summed over a. Within linear response in the bias voltage, the first-order change in the zero-temperature conductance is

$$g^{(1)} = -4\pi\ \mathrm{Im}\left\{ \mathrm{Tr}\left[r^\dagger t'\ \mathcal{V}^{2,1} \right] \right\}. \tag{9}$$

This result is valid for the general situation where quantum transport through a scatterer is modified by a weak perturbation [23]. The matrix $r^\dagger t'$ depends only on the unperturbed scatterer, while the tip's effect appears in the $\mathcal{V}$ matrix elements. The conductance change is not simply given by the current density or charge density at the tip position but is proportional to products involving a matrix element of V with two scattering states, one corresponding to an incoming electron from the left and the other from the right lead. The conductance's sensitivity to electrostatic potential variations has been considered in a one-dimensional geometry in Ref. [24]. The example of a δ-function barrier perturbed by a local tip can be analytically calculated and agrees with Eq. (9).

For a QPC, $r^\dagger t'$ is appreciable only in the vicinity of the conductance steps and is suppressed on the plateaus. A basis transformation into the eigenmodes of $t^\dagger t$ singles out the linear combinations corresponding to the modes that propagate through the constriction [16]. Only at these channels' openings is $r^\dagger t'$ significant. The first-order conductance correction [Eq. (9)] is thus the relevant term in the step regions, but to capture the plateau regions' dominant correction [25], the second-order contribution to the scattering wave functions in Eq. (4) must be taken into account. Continuing with the same method

gives the second-order conductance correction

$$g^{(2)} = -4\pi^2 \,\mathrm{Tr}\left[t^\dagger t\; \mathcal{V}^{1,2}\mathcal{V}^{2,1} + t'^\dagger t'\; \mathcal{V}^{2,1}\mathcal{V}^{1,2} + \mathrm{Re}\left\{r^\dagger t'\left(\mathcal{V}^{2,2}\mathcal{V}^{2,1} - \mathcal{V}^{2,1}\mathcal{V}^{1,1}\right)\right\}\right] . \quad (10)$$

This result, together with Eq. (9), provides the answer to the question posed in the title.

Like $g^{(1)}$, $g^{(2)}$ depends on the scattering amplitudes of the QPC and the scattering states incoming from both sides. In contrast to $g^{(1)}$, $g^{(2)}$ contains nonvanishing terms with prefactors $t^\dagger t$ and $t'^\dagger t'$. Since $r^\dagger t'$ is suppressed on the plateaus, $g^{(2)}$ is expected to be the dominant correction there. Furthermore, the second-order terms contain contributions from all effective transmitting channels, in contrast to $g^{(1)}$, which is significant only in the steps and dominated by the opening mode. Thus, the transverse shape of the channels should be observable directly with SGM on the steps without subtracting the lower mode results as done in the plateau data analysis [1].

Crucial insights into conductance quantization of a QPC have been gained through the analysis of simple models, such as the saddle potential [16] for the smooth electrostatic potential of the constriction. In addition, describing the saddle potential by a double harmonic oscillator $V(\mathbf{r}) = V_0 + \frac{M}{2}(\omega_y^2 y^2 - \omega_x^2 x^2)$ allows for an exact solution [26]. The transmission and reflection amplitudes are diagonal in the mode indices with

$$t_a = e^{-i\alpha(\mathcal{E}_a)}\left\{1 + e^{-2\pi\mathcal{E}_a}\right\}^{-1/2}$$
$$r_a = -i\, e^{-i\alpha(\mathcal{E}_a)} e^{-\pi\mathcal{E}_a}\left\{1 + e^{-2\pi\mathcal{E}_a}\right\}^{-1/2} , \quad (11)$$

where $\alpha(\mathcal{E}) = \mathcal{E} + \arg\Gamma(\frac{1}{2} + i\mathcal{E}) - \mathcal{E}\ln|\mathcal{E}|$ in terms of the dimensionless energy $\mathcal{E}_a = 2[\varepsilon - \hbar\omega_y(a + \frac{1}{2}) - V_0]/\hbar\omega_x$. In the limit $\omega_y \gg \omega_x$, a good conductance quantization is achieved [16]. As expected for an arbitrary QPC, $|r^* t|$ is appreciable only at the steps, and on the N^{th} plateau

$$\delta g \simeq g^{(2)} \simeq -8\pi^2 \sum_{a=0}^{N-1} \left|\mathcal{V}_{a,a}^{1,2}\right|^2 . \quad (12)$$

Assuming a local tip with $V(\mathbf{r}) = V_{\mathrm{T}}\delta(\mathbf{r} - \mathbf{r}_0)$ and using the semiclassical form of the scattering wavefunctions, we have

$$\mathcal{V}_{a,a}^{1,2} = \frac{V_{\mathrm{T}} l |\phi_a(y_0)|^2 t_a^*}{2\pi\hbar^2\mathcal{K}/M} \times \left\{ r_a + \exp\left[-i\left(\frac{x_0}{l}\mathcal{K} + 2\mathcal{E}_a \ln\left[\frac{\mathcal{K} + \frac{x_0}{2l}}{\sqrt{\mathcal{E}_a}}\right]\right)\right]\right\} , \quad (13)$$

for the propagating modes, where $l = \sqrt{\hbar/2M\omega_x}$ and $\mathcal{K} = \sqrt{\mathcal{E}_a + (x_0/2l)^2}$. The a^{th} eigenstate $\phi_a(y)$ of a one-dimensional harmonic oscillator with frequency ω_y yields the lobes in the transverse direction that are ubiquitous in experiments and simulations. $\mathcal{V}^{1,2}$ has real and imaginary parts that oscillate as a function of x_0 with an overall decay proportional to x_0^{-1} far from the constriction.

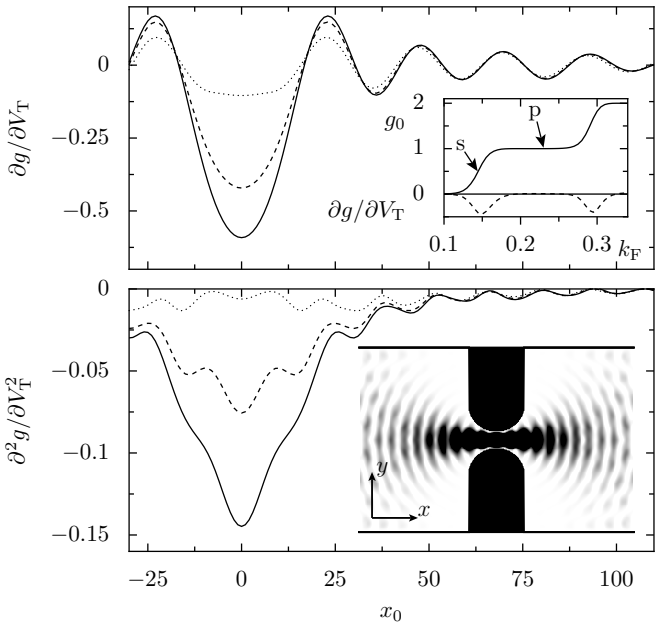

FIG. 1: Top: $\partial g/\partial V_{\mathrm{T}}$ of the conductance change with tip voltage for a hard wall QPC and a δ-tip at the first conductance step (point s of the conductance curve shown in the inset) as a function of the tip position x_0. The solid line is for $y_0 = 0$ (in the center); the dashed and dotted lines are for $y_0 = 4$ and 8, respectively. Inset: The conductance as a function of the Fermi wave vector for the unperturbed structure (solid line) and the linear correction (dashed) for $x_0 = 0$, $y_0 = 4$. Bottom: Similar, but for $\partial^2 g/\partial V_{\mathrm{T}}^2$ on the first plateau (point p). Inset: Gray-scale plot of the same data as a function of x_0 and y_0 and the configuration with a minimal width $\Delta y = 20$ used in the numerical calculations. Anderson units are used for x_0, y_0, Δy, k_{F}, and V_{T}.

The second-order correction [Eq. (12)], dominant on the plateaus, is always negative, exhibits small fringes, and has an overall decay with x_0^{-2}, in agreement with Ref. [2].

Despite the simplicity of the harmonic saddle potential and its absence of mode mixing, the results obtained are quite representative of a generic QPC's behavior. This universality stems from the above mentioned transformation into the transmission eigenmode basis, and was checked through numerical simulations in a variety of confining potentials. The results from recursive Green function algorithms [15] for the double harmonic oscillator (not shown) reproduce our analytical calculations, while those corresponding to a tight-binding model of a hard wall QPC are presented in Fig. 1. The change $\partial g/\partial V_{\mathrm{T}}$ is shown in the upper panel as a function of the tip position for a Fermi energy in the first conductance step (point s), and as a function of k_{F} in the inset. Confirming our analytical prediction, it is significant only in the step regions. The lower panel shows the change $\partial^2 g/\partial V_{\mathrm{T}}^2$ on the first plateau (point p). In agreement with Eq. (10), it is a negative correction that decreases with x_0 and y_0 further from the constriction center. The

inset shows the full dependence of $\partial^2 g/\partial V_{\rm T}^2$ on the tip position. A checkerboard pattern consistent with experimental findings [4] can be observed in the second-order correction on the first plateau. The choice of a δ tip was made for simplicity, but a smoother tip can be easily implemented.

SGM measurements can be considerably influenced by disorder near the QPC. The conductance changes [Eqs. (9) and (10)] fully incorporate the disorder through its effect on the scattering amplitudes and the scattering wave-function basis for expressing $\mathcal{V}$. The transformation in mode space that singles out the propagating modes illustrates that the conclusions regarding the relative importance of $g^{(1)}$ and $g^{(2)}$ remain valid in the presence of disorder. Since a disordered wire containing a QPC can be mapped onto an unconstrained conductor with a renormalized mean free path [27], the random-matrix theory of quantum transport [21] can be used to determine the statistical properties of the SGM patterns far from the QPC. The use of semiclassical methods [20] to evaluate the conductance corrections [Eqs. (9) and (10)] can yield an intuitive interpretation in terms of classical trajectories bridging the gap between classical [1, 2] and quantum [7–10] calculations and providing an understanding of the region near the QPC (where coherent branching and transient behaviors occur).

In summary, expressions for the lowest-order corrections to a nanostructure's conductance caused by a weak perturbation have been given. Applied to the SGM study of a QPC, the first-order corrections in the tip strength dominate at the conductance steps and are suppressed on the plateaus. The second-order corrections become dominant on the plateaus. The two expressions are of great interest since, even if most of the existing data have been obtained in the plateau regions, recent experiments [4] also explored the behavior at the mode opening finding a different interference pattern. It is also in this regime where the interaction effects [18, 19] are expected to show their signature.

The currently used tip potentials are strong enough to create a divot of depletion in the two-dimensional electron gas [1–4], which is clearly beyond the perturbative regime. However, we anticipate that much of the interpretation and many of the lessons derived from the perturbation calculations would still apply. In our quest for a rigorous interpretation of the SGM measurements, the perturbative approach is an unavoidable landmark towards the understanding of this fascinating problem. Note that in experiments on nanostructures which do not present conductance quantization, and for which therefore the linear correction [Eq. (9)] dominates the SGM response, the tip voltage has been varied over large intervals [6, 7] exhibiting the expected linear behavior.

We thank E. J. Heller, L. Kaplan, J.-L. Pichard, and C. A. Stafford for useful discussions and M. Büttiker for helpful correspondence. Financial support from the French National Research Agency ANR (Project No. ANR-08-BLAN-0030-02) and the U.S. National Science Foundation (PHY-0855337) is gratefully acknowledged. We thank the Institute for Nuclear Theory at the University of Washington for its hospitality and the DOE for partial support at the initiation of this work.

* Permanent address:Department of Physics and Astronomy, P.O. Box 642814, Washington State University, Pullman, WA 99164-2814, USA

[1] M. A. Topinka *et al.*, Science **289**, 2323 (2000).
[2] M. A. Topinka *et al.*, Nature **410**, 183 (2001).
[3] B. J. LeRoy *et al.*, Phys. Rev. Lett. **94**, 126801 (2005).
[4] M. P. Jura *et al.*, Phys. Rev. B **80**, 041303(R) (2009).
[5] R. Crook *et al.*, Phys. Rev. Lett. **91**, 246803 (2003).
[6] F. Martins *et al.*, Phys. Rev. Lett. **99**, 136807 (2007).
[7] M. G. Pala *et al.*, Phys. Rev. B **77**, 125310 (2008).
[8] G. Metalidis and P. Bruno, Phys. Rev. B **72**, 235304 (2005).
[9] A. Cresti, J. Appl. Phys. **100**, 053711 (2006).
[10] G.-P. He, S.-L. Zhu, and Z. D. Wang, Phys. Rev. B **65**, 205321 (2002).
[11] H. U. Baranger, D. P. DiVincenzo, R. A. Jalabert, and A. D. Stone, Phys. Rev. B **44**, 10637 (1991).
[12] B. J. van Wees *et al.*, Phys. Rev. Lett. **60**, 848 (1988).
[13] D. A. Wharam *et al.*, J. Phys. C: Solid State Phys. **21**, L209 (1988).
[14] L. I. Glazman, G. B. Lesovik, D. E. Khmel'nitskii, and R. I. Shekter, Pis'ma Zh. Eksp. Teor. Fiz. **48**, 218 (1988) [JETP Lett. **48**, 239 (1988)].
[15] A. Szafer and A. D. Stone, Phys. Rev. Lett. **62**, 300 (1989).
[16] M. Büttiker, Phys. Rev. B **41**, 7906(R) (1990).
[17] D. K. Ferry and R. Akis, J. Phys.: Condens. Matter **20**, 454201 (2008).
[18] A. Freyn, I. Kleftogiannis, and J.-L. Pichard, Phys. Rev. Lett. **100**, 226802 (2008).
[19] D. Weinmann, R. A. Jalabert, A. Freyn, G.-L. Ingold, and J.-L. Pichard, Eur. Phys. J. B **66**, 239 (2008).
[20] R. A. Jalabert, in *New Directions in Quantum Chaos*, ed. by G. Casati, I. Guarneri, and U. Smilansky, IOS Press Amsterdam (2000).
[21] P. A. Mello and N. Kumar, *Quantum Transport in Mesoscopic Systems*, Oxford University, New York, 2004.
[22] The x position of $\mathcal{S}_x$ is irrelevant for the final result.
[23] The conductance change is invariant under a change of current direction as well as under the changes $V(x, y) \to V(\pm x, \pm y)$ of the perturbing potential, provided the unperturbed system verifies the corresponding symmetries.
[24] V. Gasparian, T. Christen, and M. Büttiker, Phys. Rev. B **54**, 4022 (1996).
[25] The first-order correction Eq. (9) is not strictly zero on the plateaus. For infinitesimal tip strength, it remains the dominant correction, but in measurements with lab-scale tip voltages, the second-order term becomes dominant.
[26] J. N. L. Connor, Mol. Phys. **15**, 37 (1968).
[27] C. W. J. Beenakker and J. A. Melsen, Phys. Rev. B **50**, 2450 (1994).